THE JOURNAL OF BIOLOGICAL CHEMISTRY Vol. 276, No. 50, Issue of December 14, pp. 46968–46974, 2001
Printed in U.S.A.

Analysis of Integral Membrane Protein Contributions to the Deformability and Stability of the Human Erythrocyte Membrane*

Received for publication, August 15, 2001, and in revised form, October 5, 2001
Published, JBC Papers in Press, October 10, 2001, DOI 10.1074/jbc.M107855200

Heidi M. Van Dort‡, David W. Knowles§, Joel A. Chasis§, Gloria Lee§, Narla Mohandas§, and Philip S. Low‡¶

From the ‡Department of Chemistry, Purdue University, West Lafayette, Indiana 47907-1393 and the §Life Sciences Division, Lawrence Berkeley Laboratories, University of California, Berkeley, California 94720

Three major hypotheses have been proposed to explain the role of membrane-spanning proteins in establishing/maintaining membrane stability. These hypotheses ascribe the essential contribution of integral membrane proteins to (i) their ability to anchor the membrane skeleton to the lipid bilayer, (ii) their capacity to bind and stabilize membrane lipids, and (iii) their ability to influence and regulate local membrane curvature. In an effort to test these hypotheses in greater detail, we have modified both the membrane skeletal and lipid binding interactions of band 3 (the major membrane-spanning and skeletal binding protein of the human erythrocyte membrane) and have examined the impact of these modifications on erythrocyte membrane morphology, deformability, and stability. The desired changes in membrane skeletal and protein-lipid interactions were induced by 1) reaction of the cells with 4,4′-diisothiocyanostilbene-2,2′-disulfonate (DIDS), an inhibitor of band 3-mediated anion transport that dissociates band 3 into dimers (increasing its surface area in contact with lipid) and severs band 3 linkages to the membrane skeleton; 2) a fragment of ankyrin that ruptures the same ankyrin-band 3 bridge to the membrane skeleton, but drives the band 3 subunit equilibrium toward the tetramer (*i.e.* decreasing the band 3 surface area in contact with lipid); and 3) an antibody to the ankyrin-binding site on band 3 that promotes the same changes in band 3 skeletal and lipid interactions as the ankyrin fragment. We observed that although DIDS induced echinocytic morphological changes in the treated erythrocytes, it had little impact on either membrane deformability or stability. In contrast, resealing of either the ankyrin fragment or anti-band 3 IgG into erythrocytes caused spontaneous membrane fragmentation and loss of deformability/stability. Because these and other new observations cannot all be reconciled with any single hypothesis on membrane stability, we suggest that more than one hypothesis may be operative and provide an explanation of how each might individually contribute to net membrane stability.

In mechanistic models, the erythrocyte membrane is often depicted as a composite material with two coupled components surrounding a protein-rich cytoplasm. In this representation, the outer component is composed of a lipid bilayer traversed by multiple transport and structural proteins, predominantly the glycophorins and band 3. In contrast, the inner component consists of a two-dimensional scaffold of interconnecting skeletal proteins, primarily spectrin, protein 4.1R, and actin. Connections between the two components occur at regular intervals and are mainly established by bridging proteins. Prominent among the bridging proteins are ankyrin, which links the β-subunit of spectrin to the cytoplasmic domain of band 3, and protein 4.1R, which connects a spectrin-protein 4.1R-actin junctional complex to the cytoplasmic tail of glycophorin C (1). Although other proteins such as protein 4.2, dematin, p55, and adducin undoubtedly stabilize and/or regulate these bridging sites (2–11), they are not generally considered to be dominant contributors to membrane structural and mechanical properties.

Despite general agreement that the currently available models provide a broad mechanistic description of membrane shape and deformability, there are still many gaps in our understanding of the structural basis for membrane mechanical properties. In fact, a major source of uncertainty has centered on the roles of integral membrane proteins in maintaining cell shape and membrane stability. Indeed, three well articulated hypotheses are currently being discussed. In the first hypothesis, membrane-spanning polypeptides such as band 3 and glycophorin C are thought to serve primarily to anchor the protein skeleton to the lipid bilayer, thereby coupling the "stretched spring-and-girder" properties of the skeleton with the noncompressible phospholipid envelope (12). In this scenario, periodic bridges between the two layers not only force their shared morphology, but also require their stabilities to be linked via redistribution of any stress imposed on one layer into the coupled layer. A second hypothesis explaining the role of integral membrane proteins in maintaining membrane morphology/stability attributes their contribution to their ability to regulate membrane curvature (13). Due to shape and lipid packing considerations, membrane-spanning proteins are proposed to naturally impose a convex or concave bending on the surrounding lipid surface. When multiple membrane-spanning proteins with similar effects on membrane curvature are permitted to cluster, the cumulative bending is thought to ultimately drive membrane vesiculation and loss of surface area. Bridges between the membrane-spanning proteins and the spectrin skeleton are important in this model to prevent the unwanted aggregation of similarly shaped membrane proteins and the consequent vesiculation. In the third hypothesis, membrane-spanning proteins are pictured primarily as "lipid anchors" that bind and stabilize surrounding lipids and thereby prevent their spontaneous fragmentation/vesiculation (14). Evenly spaced connections to the membrane skeleton are considered

* This work was supported by National Institutes of Health Grants GM24417, HL31579, DK26263, and T32 GM08296. The costs of publication of this article were defrayed in part by the payment of page charges. This article must therefore be hereby marked "*advertisement*" in accordance with 18 U.S.C. Section 1734 solely to indicate this fact.

¶ To whom correspondence and reprint requests should be addressed. Tel.: 765-494-5273; Fax: 765-494-0239; E-mail: plow@purdue.edu.

important in this hypothesis to assure that no membrane regions become devoid of these stabilizing lipid anchors.

Although numerous mutations/perturbations have been shown to alter erythrocyte membrane stability and morphology, very few distinguish among the above three hypotheses, and those that appear to favor one hypothesis can generally be challenged by a convincing argument supporting an opposing hypothesis. For example, the claim that integral proteins function solely to couple the lipid bilayer to a more stable membrane skeleton is readily rebutted by observations showing reduced mechanical stability in membranes depleted of freely diffusing but not skeletally attached band 3 (15). Thus, in cases of hereditary spherocytosis due to a deficiency in band 3, the content of band 3 attached to the spectrin-actin skeleton is apparently normal, but the population of freely diffusing band 3 molecules is dramatically reduced. Because such erythrocytes spontaneously lose lipid bilayer until their shapes become spherical, it logically follows that the pool of free band 3 is critical to membrane morphology/stability. A contrasting conclusion is, however, suggested upon comparison of the impacts of deficiencies of various membrane-spanning proteins on membrane morphology/stability. Thus, when all 10^6 copies of band 3 are missing from the erythrocyte membrane (14, 16, 17), the membrane becomes very unstable and vesiculates in response to mechanical stress. Similarly, deletion of all 2×10^5 copies of glycophorin C leads to a related, albeit much less severe instability and elliptocytic morphology (18). However, the absence of all 10^6 copies of glycophorin A results in membranes with essentially normal morphology/stability (19). If integral proteins functioned primarily to bind and/or organize lipid, then cogent arguments must be articulated to explain why deletion of the two skeletal anchoring membrane-spanning proteins (*i.e.* band 3 and glycophorin C) has an impact on cell morphology/stability, whereas deletion of a non-anchoring membrane-spanning protein (*i.e.* glycophorin A) is phenotypically silent. Clearly, much remains to be resolved before a comprehensive understanding of the mechanistic basis of membrane morphology/stability can be achieved.

In this study, we have exploited our ability to modulate the interaction of band 3 with both the membrane skeleton and its surrounding lipids to clarify the contribution of band 3 to erythrocyte membrane stability and morphology. As discussed below, we find evidence for contributions from more than one of the above described mechanisms to the regulation of the mechanical properties of the erythrocyte membrane. We further show that these different mechanisms can compensate for each other's contributions, thereby reducing the impact of certain deleterious perturbations on membrane stability.

EXPERIMENTAL PROCEDURES

Materials—Human blood was drawn from healthy volunteers and used within 1 week of donation. DIDS,[1] EMA, and Affi-Gel 10 were obtained from Molecular Probes, Inc. Sephacryl S-200 HR and *n*-octyl β-D-glucopyranoside were from Amersham Pharmacia Biotech. $C_{12}E_8$ (octaethylene glycol dodecyl ether) was obtained from Nikko Chemical Co. ^{125}I-Bolton-Hunter reagent was from ICN. Triton X-100 was from Roche Molecular Biochemicals. Stractan was a kind gift of Martin Sorrette. All other reagents were obtained from major suppliers and were of the highest purity available.

Ankyrin Fragment Purification—A 45.6-kDa fragment of ankyrin containing the binding site for band 3 (residues 403–827) was expressed in *Escherichia coli* strain BL21(DE3)/pLysS (the expression vector was a kind gift of Dr. Vann Bennett) and purified as described by Davis and Bennett (1). The purified protein was concentrated and stored at 4 °C until used. The protein was found to remain stable and functional up to 1 year in high ionic strength gel filtration buffer (10 mM sodium phosphate, 1 M sodium bromide, 1 mM EDTA, 1 mM sodium azide, and 1 mM dithiothreitol, pH 7.4). Just prior to use, however, the buffer was changed to isotonic phosphate buffer because the ankyrin fragment was stable for only 7 days in low ionic strength solutions. Ankyrin fragment concentration was determined from its absorbance at 280 nm (21) using an experimentally determined $\epsilon = 15{,}816\ M^{-1}\ cm^{-1}$ for the 45.6-kDa protein, which calculates to 0.347 ml $mg^{-1}\ cm^{-1}$.

IgG Purification—Generation of antibodies against an ankyrin-binding region of the cytoplasmic domain of band 3 (residues 190–203, PQHSSLETQLFCGQ) was carried out as described previously by Willardson *et al.* (22). Purification of the antibodies from the defibrinated rabbit antiserum was achieved by precipitation with cold 40% NH_4SO_4, pH 7.5. After resolubilizing in PBS, the antibody solution was dialyzed first against PBS and then against 100 mM MOPS, pH 6.5. The antibodies were loaded onto an affinity column prepared by coupling the above peptide to Bio-Rad Affi-Gel 10 beads, eluted with 1.0 M propionic acid, and immediately brought to neutral pH with NH_4OH. The purified antibodies were concentrated and dialyzed against PBS. Because the antibodies were stable for only 3 days in low ionic strength buffers, the buffer was changed to lysis buffer by ultrafiltration immediately prior to use.

Labeling of Band 3 with DIDS and EMA—Washed red cells (50% hematocrit) were incubated with 50 μM DIDS for 1 h at 37 °C in 0.15 M NaCl and 5 mM sodium phosphate, pH 7.4. Cells were washed four times with 5 volumes of the same buffer containing 1% bovine serum albumin to remove unreacted DIDS and then three times without the serum albumin. Under these conditions, >95% of the DIDS resides on band 3 (23).Washed red cells (20% hematocrit) were incubated with 0.1 μM EMA for 1 h at 25 °C in 0.15 M NaCl and 5 mM sodium phosphate, pH 7.4. Cells were washed four times with 5 volumes of the same buffer containing 1% bovine serum albumin to remove unreacted EMA and then three times without the serum albumin. Under these conditions, >80% of the EMA resides on band 3 (24, 25).

Analysis of Band 3 Retention in Membrane Skeletons—Erythrocytes were digested with 1 mg/ml chymotrypsin at 37 °C for 1 h to cleave band 3 into its non-glycosylated 65,000-Da and heterogeneously glycosylated 35,000-Da fragments. This cleavage does not impact on anion transport or membrane skeletal interactions (23), but allows sharper resolution of the 65,000-Da fragment of band 3 by SDS-polyacrylamide gel electrophoresis. To evaluate the amount of band 3 retained in the membrane skeletons, 1 ml of packed DIDS-treated, untreated, or resealed spherocytic cells that had been separated from vesiculated membrane components was treated with 1 ml of 4% *n*-octyl β-D-glucopyranoside supplemented with 0.5 mM dithiothreitol, 20 μg/ml leupeptin, 20 μg/ml pepstatin A, 1 mM EDTA, and 80 μg/ml phenylmethanesulfonyl fluoride. The resulting membrane skeletal extract was loaded onto a 35% sucrose cushion, and the sample was centrifuged at 85,500 × *g* for 90 min to separate the solubilized membrane components from the pelleted membrane skeletons. The tubes were inverted to allow the supernatant to drain, and the pellet was solubilized in SDS buffer and analyzed by SDS-polyacrylamide gel electrophoresis. Band 3 content in the membrane skeletons was easily quantitated by densitometric analysis of the well defined 65,000-Da fragment.

Fluorescence-imaged Microdeformation Assay—Band 3 association with the membrane skeleton in intact membranes was evaluated using the micropipette aspiration technique of Evans *et al.* (27) coupled with fluorescence imaging (28, 29). In this method, band 3 was fluorescently labeled in intact cells with 0.1 μM EMA or 50 μM DIDS prior to resealing with the ankyrin fragment, anti-band 3 IgG, or ovalbumin (as a non-interacting control). After varying periods of incubation at 37 °C, the redistribution of band 3 relative to lipids and the membrane skeletal component actin was evaluated following aspiration of part of the membrane into a 1–1.2-μm diameter micropipette. As described elsewhere (27, 29), the aspirated membrane surface that entered the pipette formed a cylindrical projection with a hemispherical cap at the tip, whereas the remaining red cell formed a sphere outside of the pipette. The distribution of band 3 along the projection, as determined by the fluorescence of EMA or DIDS, was compared with the distribution of a freely diffusing lipid probe (fluorescein-labeled phosphatidylethanolamine) and a marker of the membrane skeleton (phalloidin-labeled actin). Fluorescence intensity was quantified using a Nikon Diaphot microscope with a liquid nitrogen-cooled camera (CH-260, Photometrics Ltd., Tucson, AZ) as described by Hiraoka *et al.* (30). The means ± S.D. of the band 3 density gradients were derived from multiple experiments and several samplings of the labeled cells.

Ektacytometry—Membrane deformability and stability were measured using an ektacytometer (31–33). Whole cells were suspended in

[1] The abbreviations used are: DIDS, 4,4′-diisothiocyanostilbene-2,2′-disulfonate; EMA, eosin-5-maleimide; PBS, phosphate-buffered saline; MOPS, 3-(*N*-morpholino)propanesulfonic acid.

TABLE I
Effect of different variables on the concentration gradient of band 3 and other membrane components along a membrane projection aspirated into a micropipette

Fluorescent label	Time	Micropipette density gradient
	h	
EMA-labeled band 3 (control)	1–12	0.12 ± 0.02
DIDS-labeled band 3	1	0.07 ± 0.01
DIDS-labeled band 3	12	0.06 ± 0.02
EMA-labeled band 3 + 9 μM ankyrin fragment	1–2	0.10 ± 0.02
EMA-labeled band 3 + 17.5 μM ankyrin fragment	1–2	0.00 ± 0.01
Rhodamine/phalloidin-labeled actin		0.15 ± 0.02
Fluorescein-labeled phosphatidylethanolamine		0.00

PBS containing 4% polyvinylpyrrolidone or 25% dextran (cell deformability analysis), and resealed ghosts were suspended in PBS containing 35% dextran (membrane mechanical stability analysis) or in PBS containing 40% stractan (membrane deformability analysis) and deformed in a Couette viscometer, in which the outer cylinder is spun to produce a uniform shear stress. For deformability analyses, erythrocytes were subjected to increasing shear stresses in a laminar flow field, which caused the discoid cells to deform into ellipsoids. For stability analyses, resealed erythrocyte membranes were subjected to a constant higher shear stress, which caused fragmentation of the cells, generating small spherical vesicles. A laser beam was diffracted by the cells in the sample, and the diffraction pattern was analyzed to obtain quantitative information about the deformation of the sheared cells. Quantitation of the ellipticity of the pattern was graphically recorded as the deformability index as a function of applied shear stress for deformability measurements and as a function of time for membrane mechanical stability measurements. To measure deformability and mechanical stability, the cells were subjected to shear stresses of 0–125 and 575 dynes/cm^2, respectively, over a 3-min period.

Resealing Studies—Freshly drawn erythrocytes were washed three times with PBS, lysed in cold hypotonic buffer (7.5 mM NaH_2PO_4 and 1 mM MgATP, pH 7.4) at 20% hematocrit, and then incubated on ice for 30 min. Protein solutions containing either the ankyrin fragment or anti-band 3 IgG were aliquoted into a 150-μl total volume and also incubated on ice for 30 min to ensure that all samples were equilibrated at 0 °C. Then, 30 μl of packed leaky ghosts were added to the desired protein solution, gently agitated to promote equilibration of the protein into the cells, and allowed to sit for 1 h. At that time, 18.2 μl of a 10× stock of PBS were added and gently mixed, and the suspension was incubated at 37 °C for 30 min to reseal the membranes. As resealing of the ankyrin fragment or anti-band 3 antibody into the fresh erythrocytes led to a progressive loss of membrane surface, the residual cells were separated from the membrane vesicles by centrifugation at 13,000 × *g* for 10 min. Under these conditions, the larger spherocytic and stomatocytic cells pelleted to the bottom of the centrifuge tube, and the vesicles remained in the supernatant.

Quantitation of the amount of the 45.6-kDa ankyrin fragment associated with the erythrocyte membranes following lysis and resealing was determined by comparing the amount of ^{125}I-ankyrin fragment and ^{125}I-ovalbumin (both labeled with ^{125}I-Bolton-Hunter reagent) (34) retained on the membranes of the resealed cells. After removal of unbound protein, the resealed cells were relysed and washed three times with ice-cold 5 mM sodium phosphate and 1 mM EDTA, pH 7.5. The total protein content of the washed membranes was then determined, and the amount of specifically bound protein was evaluated using a γ-counter (Packard Instrument Co.). A similar strategy was employed for the fluorescence-imaged microdeformation studies, except that a fluorescein isothiocyanate-labeled ankyrin fragment was introduced during the resealing step.

To determine whether the 45.6-kDa ankyrin fragment could displace whole ankyrin from red cell membranes, 45.6-kDa ankyrin was incubated at 100-fold molar excess with inside-out vesicles (spectrin- and actin-depleted membrane vesicles) at 25 °C for 24 h. Briefly, erythrocytes were lysed with 5 mM sodium phosphate and 1 mM EDTA, pH 7.4; and spectrin and actin were removed by incubating the membranes in a 10-volume excess of 0.5 mM EDTA, pH 8.0, at 37 °C for 20 min. The resulting inside-out vesicles were washed and incubated with the added protein in 5% sucrose, 50 mM sodium phosphate, 50 mM boric acid, 30 mM NaCl, 1 mM EDTA, and 0.2 mM dithiothreitol adjusted to pH 7.8 or in 5 mM sodium phosphate, 1 mM EDTA, 0.5 mM diisopropyl fluorophosphate, 20 μg/ml pepstatin, and 20 μg/ml leupeptin, pH 7.4. The unbound protein was separated from the inside-out vesicles by pelleting the inside-out vesicles through 1 ml of a 25% sucrose cushion at 19,000 × *g* for 15 min. Quantitation of the residual bound ankyrin was accomplished by densitometry of the pellet following its separation in the 3.5–8% electrophoretic gel system of Fairbank *et al.* (35).

RESULTS

Effect of Band 3 Perturbations on Its Retention in Membrane Skeletons—DIDS is an inhibitor of anion transport that reacts with lysine 539 in the membrane-spanning domain of band 3 (23). DIDS binding to band 3 has been shown to induce loss of all low affinity and roughly half of all high affinity ankyrin-binding sites on the membrane (36), and it thereby reduces band 3 retention in membrane skeletons prepared directly from DIDS-labeled cells by ~50% (36). DIDS treatment therefore constitutes a noninvasive method by which the major bilayer-skeleton bridge can be severed and its impact on membrane stability examined. Analysis of the DIDS-labeled cells employed in this study revealed a reduction in the skeletally linked band 3 content of ~45% within 1 h of DIDS labeling in four separate skeleton preparations (data not shown). Thus, extraction of the modified cells directly in 2% *n*-octyl β-D-glucopyranoside yielded spectrin-actin skeletons with only approximately on-half of their normal band 3 content. Similar methods of analysis demonstrated that resealing the 45.6-kDa ankyrin fragment (8.8 μM) into erythrocytes caused a similar (~45%) loss of band 3 from the corresponding *n*-octyl β-D-glucopyranoside-extracted skeletons. Dissociation of band 3 from the membrane skeleton by the 45.6-kDa ankyrin fragment was expected because it competes with endogenous ankyrin for band 3 binding, but lacks the complementary domain for spectrin binding (37).

Evaluation of Band 3 Skeletal Attachment Using a Fluorescence-imaged Microdeformation Assay—To confirm that the band 3 linkage to the membrane skeleton was at least partially disrupted by both DIDS derivatization and ankyrin fragment incorporation, the distribution of band 3 relative to both the membrane skeleton and a fluid lipid marker was quantitated during aspiration of a region of the erythrocyte membrane into a 1–1.2-μm diameter micropipette. Band 3 distribution in DIDS-labeled cells could be directly monitored because DIDS is fluorescent. However, band 3 distribution in both unmodified and ankyrin fragment-containing cells was determined using EMA-labeled cells (24, 25). EMA fluorescently labels band 3 without disrupting its interactions with other proteins (data not shown). Because unmodified band 3 is composed of both skeletally associated and freely diffusing components, it would be expected to exhibit a redistribution pattern that is intermediate between those of the fluid-phase lipid marker and the immobile membrane skeleton. As anticipated, EMA-labeled band 3 in control cells did indeed migrate with a density gradient of 0.12, which is intermediate between that of skeletally attached phalloidin-labeled actin (0.15) and freely diffusing lipid (0.0) (Table I). In contrast, when band 3 was labeled with DIDS, the density gradient was more gradual, as visualized by the fluorescence intensity profile (Fig. 1) and as quantitated in

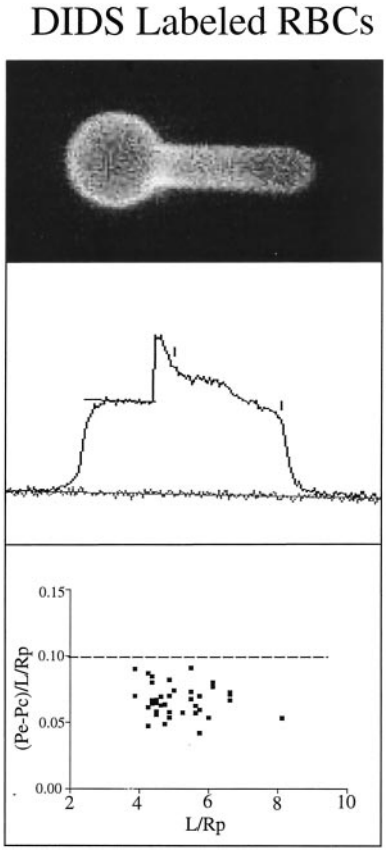

FIG. 1. **Membrane microdeformation analysis of the impact of DIDS labeling on the association of band 3 with the membrane skeleton.** A fluorescence micrograph (*upper panel*) and the corresponding intensity profile (*middle panel*) of DIDS-labeled band 3 in an erythrocyte membrane are shown. The intensity profile was plotted as relative fluorescence intensity (*ordinate*) *versus* distance along the deformation axis (*abscissa*). *Pe* is the relative fluorescence intensity of the membrane at the entrance of the pipette, and *Pc* is the relative fluorescence intensity at the cap of the cell projection in the pipette. The average density gradient, $(Pe - Pc)/L/Rp$, was plotted *versus* the aspiration length (L) scaled by the pipette radius (Rp), L/Rp, for 40 aspirated cells (*lower panel*). The average density gradient for DIDS-labeled band 3 was less than that of EMA-labeled band 3 indicated by the *dotted line*. *RBCs*, red blood cells.

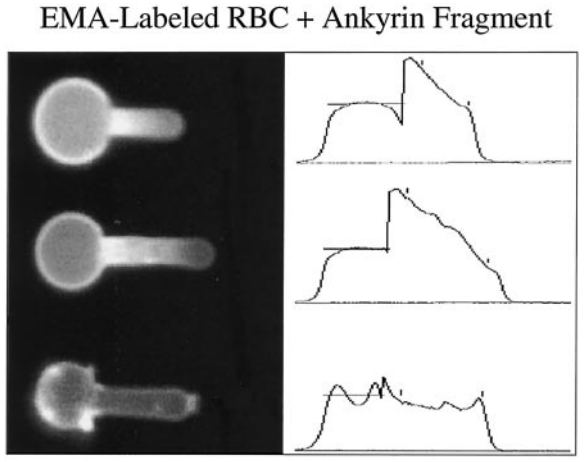

FIG. 2. **Membrane microdeformation analysis of the impact of resealing the 45.6-kDa ankyrin fragment into lysed erythrocytes on the association of band 3 with the membrane skeleton.** Shown are fluorescence micrographs (*left panels*) and the corresponding intensity profiles (*right panels*) of EMA-labeled band 3 in erythrocyte membranes resealed with no ankyrin fragment (*upper panels*), 9 μM ankyrin fragment (*middle panels*), or 17.5 μM ankyrin fragment (*lower panels*). The intensity profiles were plotted as relative fluorescence intensity (*ordinate*) *versus* distance alone the deformation axis (*abscissa*). The results indicate that binding of unlabeled ankyrin fragment to the erythrocyte membrane alters the average EMA-labeled band 3 density gradient. A markedly decreased EMA-labeled band 3 gradient and cell fragmentation were noted at an ankyrin fragment concentration of 17.5 μM (*lower panel*). *RBC*, red blood cell.

the derived density gradient (Table I). These data imply that DIDS-labeled band 3 associates less with the membrane skeleton compared with EMA-labeled band 3. This result is consistent with the reduced retention of DIDS-labeled band 3 in detergent-extracted membrane skeletons.

Incorporation of the 45.6-kDa ankyrin fragment into EMA-labeled cells caused a concentration-dependent release of band 3 from membrane skeletal constraints (Fig. 2 and Table I). Thus, as the concentration of entrapped fragment was increased from 0 to 9 and 17.5 μM, the concentration gradient of band 3 along the aspirated membrane decreased from 0.12 to 0.10 and 0.00, respectively. At the highest fragment concentration, band 3 was nearly completely dissociated from the underlying skeleton and appeared to be as diffusible as membrane lipids. In contrast, incorporation of the ankyrin fragment had no effect on the actin gradient (data not shown). Taken together with the biochemical compositional analyses described above, we conclude that both DIDS labeling of band 3 and ankyrin fragment incorporation reduce the number of band 3 bridges to the membrane skeleton.

Effect of DIDS Labeling and Ankyrin Fragment Incorporation on the Dimer-Tetramer Subunit Equilibrium in Band 3—Because lipid binding is hypothesized to constitute one mechanism by which integral membrane proteins maintain membrane stability (14) and because more protein surface becomes available for lipid binding when band 3 dissociates from a tetramer to dimer, it was also important to examine the impact of DIDS and 45.6-kDa ankyrin binding on the band 3 dimer-tetramer equilibrium. In this regard, we have already shown that DIDS labeling of whole erythrocytes shifts the band 3 subunit dissociation equilibrium strongly toward the dimer (36). However, because these earlier studies were conducted under different incubation conditions, DIDS-labeled samples prepared identically to those used in the present micromechanical study (see below) were examined for their band 3 dimer/tetramer ratios. By 1 h after DIDS labeling, the dimer/tetramer ratio, measured by quantitative high pressure liquid chromatography, had increased from ~1.5 to ~6. Thus, in addition to promoting decreased membrane-to-skeleton linkages, DIDS likely increases the interaction of band 3 with membrane lipid by dissociating some of the tetramer species to dimers.

A related analysis was also conducted on 45.6-kDa ankyrin fragment-loaded cells. However, unlike DIDS (36), the ankyrin fragment was found to promote band 3 self-association. At the lower fragment concentration of ~9 μM, the dimer/tetramer ratio was ~0.5. At the higher concentration of 17.5 μM, the ratio was <0.2. Thus, although both DIDS and 45.6-kDa ankyrin sever membrane-to-skeleton linkages, they shift the band 3 subunit equilibrium in opposite directions, presumably changing the fraction of protein-stabilized lipid also disparately.

Visualization of the Cell Morphology of DIDS-labeled and 45.6-kDa Ankyrin Fragment-treated Cells—Because much can be learned regarding induced membrane structural changes by visual inspection of modified erythrocytes, we compared the morphologies of DIDS-labeled, 45.6-kDa ankyrin-treated, and control cells by light microscopy. When either ovalbumin (data not shown) or no protein (Fig. 3*A*) was resealed into red cells, the resulting erythrocytes displayed a normal discoid shape.

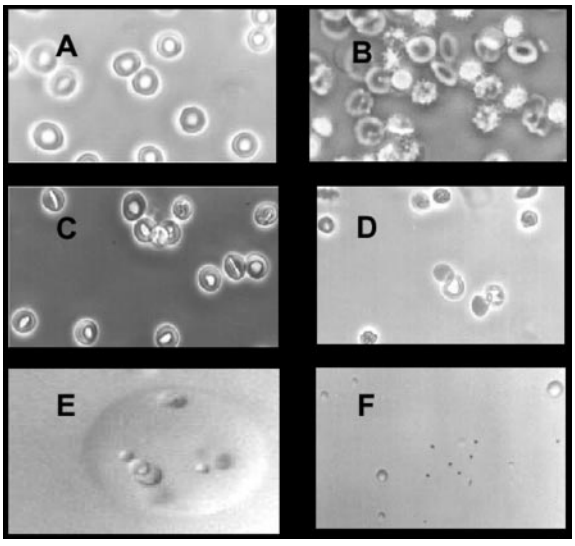

FIG. 3. **Impact of DIDS labeling and ankyrin fragment incorporation on the morphology of human erythrocytes.** Fresh human erythrocytes were either labeled with 50 μM DIDS (*B*) or lysed in cold hypotonic buffer and resealed with 0 μM (*A*), 8.8 μM (*C*), 13.2 μM (*D*), 17.5 μM (*E*), or 26.4 μM (*F*) ankyrin fragment. Cells were then fixed and viewed under a light microscope as described under "Experimental Procedures." Note that at increasing ankyrin fragment concentrations, the cells spontaneously deformed and ultimately fragmented into smaller vesicles.

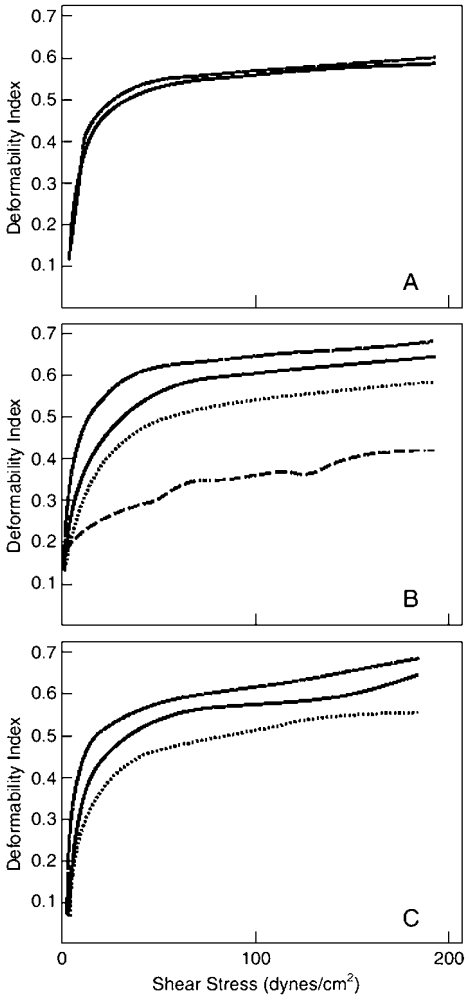

FIG. 4. **Effects of DIDS labeling, ankyrin fragment incorporation, and anti-band 3 incorporation on the deformability of human erythrocyte membranes.** *A*, erythrocytes were labeled with DIDS and prepared for ektacytometry as described under "Experimental Procedures." Unlabeled or EMA-labeled membranes (*upper curve*) and DIDS-labeled membranes (*lower curve*) all deformed upon exposure to increasing levels of applied shear stress to a similar extent and with similar kinetics. *B*, lysed erythrocytes were resealed in the presence of 8.8 μM (*first curve*), 0 μM (*second curve*), 13.2 μM (*third curve*), or 17.5 μM (*fourth curve*) ankyrin fragment and subjected to increasing levels of applied shear stress in the ektacytometer. Deformability was analyzed as described under "Experimental Procedures." The dramatic loss of deformability at high ankyrin fragment content is likely a consequence of membrane fragmentation and loss of surface area. *C*, lysed erythrocytes were resealed in the presence of 0 μM (*first curve*), 0.33 μM (*second curve*), or 0.53 μM (*third curve*) anti-band 3 IgG and examined for changes in deformability as described for *B*.

However, modification of the intact red cells with DIDS caused most of the cells to become echinocytic (Fig. 3*B*). In contrast, at low ankyrin fragment concentrations (8–11 μM), the cells became strikingly stomatocytic (Fig. 3*C*), whereas at intermediate ankyrin concentrations (13–18 μM), the cells assumed a more crinkled but stomatocytic shape, with small membrane vesicles appearing within the cytosol (Fig. 3, *D* and *E*). At the highest ankyrin fragment concentration (26.4 μM), the cells spontaneously fragmented, yielding a few small spherocytic cells and a large population of membrane vesicles (Fig. 3*F*). Although the majority of morphological changes were complete within a few minutes, minor changes could often be observed for up to 1 h. These data suggest that the 45.6-kDa ankyrin fragment and DIDS have very different effects on membrane morphology and stability, despite their similar influences on membrane-to-skeleton linkages.

Effect of DIDS Labeling and 45.6-kDa Ankyrin Fragment Treatment on the Deformability of Human Erythrocytes—To determine how modification with DIDS might impact on erythrocyte deformability, erythrocytes were labeled with DIDS or EMA or left unlabeled and then incubated at 37 °C for various periods of time and mechanically stressed in a laminar flow field in an ektacytometer. Unlabeled and EMA-derivatized cells displayed the same deformability profiles under applied shear stress as freshly isolated cells (data not shown). Surprisingly, DIDS-derivatized samples also exhibited an essentially normal deformability profile (Fig. 4*A*). Thus, despite the ability of DIDS to sever skeleton linkages and to dissociate band 3 tetramers to dimers, DIDS does not appear to alter erythrocyte membrane deformability

A significantly different response was observed when the 45.6-kDa ankyrin fragment was resealed into transiently lysed erythrocytes. Although resealed cells containing either no exogenous protein or ovalbumin (inert control) were found to deform normally (Fig. 4*B*, *second curve*), resealed cells containing relatively low ankyrin fragment concentrations (8–11 μM) displayed a slightly elevated deformability index (*first curve*), suggesting that they are more deformable than normal. At a still higher ankyrin fragment concentration (13.2 μM), gradual spontaneous membrane vesiculation occurred, leading to release of small spherical vesicles that could not deform in the ektacytometer. As a consequence, a moderate decline in deformability index ensued (*third curve*). At the highest ankyrin concentration tested (17.6 μM), the resealed cells fragmented so rapidly that only non-deformable vesicles remained (*fourth curve*).

Because we had access to a small amount of purified antibody (polyclonal IgG) directed against an ankyrin-binding sequence on band 3 (residues 190–203) and because this antibody had been previously shown to compete with intact ankyrin for its membrane attachment site (22), we also examined the effect of anti-band 3 antibody on the morphology and deformability of the resealed cells. Entrapment of anti-band 3 antibody into resealed cells yielded cells that behaved similarly to 45.6-kDa

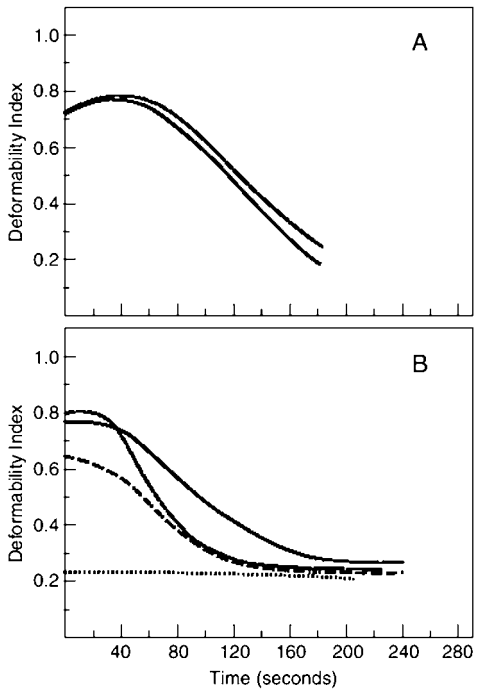

FIG. 5. **Effect of DIDS labeling and ankyrin fragment incorporation on membrane mechanical stability as assayed by ektacytometry.** *A*, erythrocytes were labeled with DIDS (*lower curve*) or left unlabeled (*upper curve*) and analyzed for changes in deformability index as a function of time at a constant value of applied shear stress in the ektacytometer as described under "Experimental Procedures." Cells resealed with either no protein or the non-interacting protein ovalbumin showed similar fragmentation profiles. *B*, erythrocytes were resealed in the presence of 8.8 μM (*first curve* on the *y axis*), 0 μM (*second curve*), 17.5 μM (*third curve*), or 26.4 μM (*fourth curve*) ankyrin fragment and subjected to a constant value of applied shear stress in the ektacytometer. Deformability was again recorded as a function of time.

ankyrin-loaded cells. Thus, at both 0.33 and 0.53 μM IgG, the IgG-treated erythrocytes displayed a marked decrease in deformability (Fig. 4*C*). At still higher IgG concentrations, the resealed erythrocytes spontaneously fragmented before they could be analyzed by ektacytometry, *i.e.* similar to cells resealed with 17.5 μM 45.6-kDa ankyrin fragment. Although inadequate quantities of antibody prohibited more detailed analyses, we speculate that the resealed IgG was able to displace endogenous ankyrin and to cross-link band 3 in a manner similar to that of the ankyrin fragment.

Analysis of Treated Cells for Changes in Membrane Mechanical Stability—The mechanical stability of a membrane can be evaluated by measuring the rate at which it fragments during exposure to a constant elevated shear stress. Importantly, this fragmentation process can be monitored with an ektacytometer by recording the rate of decrease in the deformability index as the cell fragments to non-deformable vesicles at high shear stress. Thus, to characterize the stability of the DIDS-labeled and 45.6-kDa ankyrin fragment-treated membranes more thoroughly, erythrocytes treated as outlined above were compared for their abilities to withstand high levels of applied shear stresses. As shown in Fig. 5*A*, erythrocytes that were either left unlabeled or labeled with DIDS or erythrocytes that contained either no protein or ovalbumin resealed inside showed identical stability profiles at all time points during multiple experiments. Even at very high shear stresses, DIDS-labeled membranes exhibited normal stability.

In contrast, resealing the ankyrin fragment at concentrations up to 11 μM caused the resealed ghosts to become initially more deformable (as indicated by the initial increase in the deformability index) and then to rapidly fragment (as indicated by the faster decline in the deformability index compared with the control) (Fig. 5*B*). At 17.5 μM fragment, the cells were already vesiculating even at the earliest time point, as depicted by the lower initial deformability index. At still higher concentrations, the ghosts completely disintegrated before any fluid shear stress could be applied and therefore could not be deformed in the ektacytometer (Fig. 5*B*). Thus, in terms of membrane stability, the DIDS-labeled erythrocytes once again exhibited a very different pattern compared with the ankyrin fragment-treated cells.

Concentration Dependence of 45.6-kDa Ankyrin Fragment Incorporation into Erythrocytes—Using ^{125}I-Bolton-Hunter-labeled ankyrin fragment, it was possible to estimate the number of ankyrin fragments retained in the cell at each bulk fragment concentration. At 11 μM bulk ankyrin fragment, where mechanical deficiencies were first emerging, but morphological abnormalities were already apparent, approximately one fragment was encapsulated per 3.5 molecules of band 3. At 17.5 μM bulk ankyrin, where the membrane mechanical abnormalities had become unequivocal, the ratio was closer to 1:2. Although we could not establish that this entrapped fraction was entirely membrane-bound, because ^{125}I-ovalbumin was retained at $<$10% of the efficiency of the ankyrin fragment, we hypothesize that most of the 45.6-kDa ankyrin must have been associated with specific sites on the membrane.

DISCUSSION

We have shown by two independent methods that both DIDS labeling and 45.6-kDa ankyrin fragment binding sever ankyrin-band 3 linkages connecting the membrane to its spectrin skeleton. Thus, both treatments reduce the fraction of band 3 retained in *n*-octyl β-D-glucopyranoside-extracted membrane skeletons, and both perturbations increase the lateral mobility of band 3 in the membrane. If membrane stability were predominantly regulated by the number of membrane-to-skeleton linkages, both modifications would be expected to destabilize the membrane. However, no significant change in either mechanical stability or deformability was observed in the DIDS-labeled samples, whereas a dramatic decrease in both stability and deformability was invariably observed in the fragment-treated cells. Based on these data, one must conclude that factors other than the number of membrane-to-skeleton tethers can influence the mechanical properties of the human erythrocyte membrane.

In search of other possible contributors to erythrocyte membrane mechanical stability, we also examined the impact of DIDS and ankyrin fragment binding on the oligomeric state of band 3. Our motivation to explore this self-association equilibrium stemmed from the fact that two of the three aforementioned models of membrane stability (see the Introduction) predict destabilization of the bilayer whenever an integral membrane protein as abundant as band 3 begins to aggregate. The lipid anchor hypothesis anticipates membrane destabilization during protein self-association because less protein surface area becomes available for lipid binding. The membrane curvature hypothesis predicts bilayer fragmentation because colocalization of multiple wedge- or cone-shaped proteins can force a localized bilayer curvature that leads to vesiculation. Congruent with both models, 45.6-kDa ankyrin binding was found to promote band 3 association, whereas DIDS labeling was seen to induce disaggregation.

Although the strong destabilizing effects of ankyrin fragment incorporation support a structural function for band 3 beyond its role as a skeletal anchor, the lack of any significant effect of DIDS on membrane mechanical properties also argues that neither the membrane curvature nor lipid anchor hypothesis is fully capable of explaining all mechanical properties of the membrane. Thus, both hypotheses predict that DIDS-in-

duced dissociation of band 3 tetramers to dimers should stabilize the bilayer. The lipid anchor hypothesis would attribute the anticipated enhanced stability to increased lipid binding, whereas the membrane curvature hypothesis would ascribe the same stabilization to further delocalization of a curvature-inducing element, *i.e.* band 3. However, DIDS does not enhance membrane stability. Therefore, to reconcile this observation with the membrane curvature and lipid anchor hypotheses, one would have to postulate that the predicted stabilization does occur, but that it is somehow offset by an independent DIDS-induced destabilization. Such destabilization probably derives from rupture of ~50% of the membrane-to-skeleton tethers, as proposed by the "skeleton bridge" hypothesis and supported by observations on *nb/nb* mice. Thus, erythrocytes from these anemic mice lack ankyrin; and even though their band 3 elutes almost exclusively as a dimer during size-exclusion chromatography, their membranes are extremely unstable (20). Consistent with this interpretation, we have noted that most of the membrane mechanical deficiencies in our studies were manifested at ankyrin fragment concentrations above ~9 μM (Figs. 4*B* and 5*B*), where rupture of membrane-to-skeleton bridges becomes prominent (Table I), but ankyrin fragment-induced tetramerization of free (dimeric) band 3 is probably already complete. Taken together, we do not believe that any single hypothesis of membrane stability can account for all of the mechanical properties of the erythrocyte membrane reported to date.

What model of membrane mechanical stability then appears to be most valid, and which experimental observations must any model of erythrocyte membrane stability adequately explain? We would suggest that any all-inclusive model of membrane stability must be able to accommodate at least the following observations. (i) A large reduction in the content of freely diffusing band 3 without any diminution of the normal complement of skeletally anchored band 3 leads to membrane instability and hereditary spherocytosis (15). (ii) Rupture or deletion of all ankyrin-band 3 bridges results in extremely fragile erythrocytes (12, 14, 16, 17). (iii) Rupture of most glycophorin C-protein 4.1-spectrin/actin bridges causes no measurable change in membrane stability (26) (iv) Elimination of all ~10^6 copies of glycophorin A induces no phenotypic change in the affected erythrocytes (19), whereas elimination of all copies of band 3 or ankyrin yields very unstable cells (14, 16, 17, 20). (v) Dissociation of half of the ankyrin-band 3 bridges by DIDS labeling causes no change in membrane mechanical stability, whereas severance of a similar fraction of ankyrin bridges by the truncated ankyrin leads to spontaneous membrane vesiculation. Because no single model of membrane stability can explain all of these observations, it seems likely to us that (i) membrane-to-skeleton tethers, (ii) protein-induced membrane curvature, (iii) protein-lipid interactions, and perhaps still other factors yet to be identified can all contribute to the net stability of the erythrocyte membrane. As simple as the red cell is, it may still require considerable scrutiny before its most fundamental characteristics are fully understood.

Acknowledgments—We thank Drs. James Salhany and Dennis Discher for helpful scientific discussions.

REFERENCES

1. Davis, L., and Bennett, V. (1990) *J. Biol. Chem.* **265,** 10589–10596
2. Snyers, L., Thines-Sempoux, D., and Prohaska, R. (1997) *Eur. J. Cell Biol.* **73,** 281–285
3. Sinard, J. H., Stewart, G. W., Argent, A. C., and Morrow, J. S. (1994) *Mol. Biol. Cell* **5,** 421a (abstr.)
4. Gilligan, D. M., and Bennett, V. (1993) *Semin. Hematol.* **30,** 74–83
5. Rybicki, A. C., Heath, R., Lubin, B., and Schwartz, R. S. (1988) *J. Clin. Invest.* **81,** 255–260
6. Cohen, A. M., Liu, S.-C., Derick, L. H., and Palek, J. (1986) *Blood* **68,** 920–926
7. Maksymiw, R., Sui, S.-F., Gaub, H., and Sackmann, E. (1987) *Biochemistry* **26,** 2983–2990
8. Bourguignon, L. Y. W., Walker, G., Suchard, S., and Balazovich, K. (1986) *J. Cell Biol.* **102,** 2115–2124
9. Kalomiris, E., and Bourguignon, L. Y. W. (1988) *J. Cell Biol.* **106,** 319–327
10. Lokeshwar, V. B., Fregien, N., and Bourguignon, L. Y. W. (1994) *J. Cell Biol.* **126,** 1099–1109
11. Davis, J. Q., and Bennett, V. (1990) *J. Biol. Chem.* **265,** 17252–17256
12. Low, P. S., Willardson, B. M., Mohandas, N., Rossi, M., and Shohet, S. (1991) *Blood* **77,** 1581–1586
13. Morrow, J. S., Rimm, D. L., Kennedy, S. P., Cianci, C. D., Sinard, J. H., and Weed, S. A. (1997) in *Handbook of Physiology*, (Hoffman, J., and Jamieson, J., eds) pp. 485–540, Oxford University Press, London
14. Peters, L. L., Shivdasani, R. A., Liu, S.-C., Hanspal, M., John, K. H., Gonzalez, J. M., Brugnara, C., Gwynn, G., Mohandas, N., Alper, S., Orkin, S. H., and Lux, S. E. (1996) *Cell* **86,** 917–927
15. Jarolim, P., Rubin, H. L., Liu, S.-C., Cho, M. R., Brabec, V., Derick, L. H., Yi, S. J., Saad, S. T. O., Alper, S., Brugnara, C., Golan, D. E., and Palek, J. (1994) *J. Clin. Invest.* **93,** 121–130
16. Inaba, M. Yawata, A., Koshino, I., Sato, K., Takeuchi, M., Takakuwa, Y., Manno, S., Yawata, Y., Kanzaki, A., Sakai, J., Ban, A., Ono, K., and Maede, Y. (1996) *J. Clin. Invest.* **97,** 1804–1817
17. Southgate, C. D., Chishti, A. H., Mitchell, B., Yi, S. J., and Palek, J. (1996) *Nat. Genet.* **14,** 227–230
18. Reid, M., Chasis, J., and Mohandas, N. (1987) *Blood* **69,** 1068–1072
19. Tanner, M. J., and Anstee, D. J. (1976) *Biochem. J.* **153,** 271–277
20. Yi, S. J., Liu, S.-C., Derick, L. H., Murray, J., Barker, J. E., Cho, M. R., Palek, J., and Golan, D. E. (1997) Biochemistry **36,** 9596–9604
21. Pace, C. N., Vajdos, F., Fee, L., Grimsley, G., and Gray, T. (1995) *Protein Sci.* **4,** 2411–2423
22. Willardson, B. M., Thevenin, B. J.-M., Harrison, M. L., Kuster, W. M., Benson, M. D., and Low, P. S. (1989) *J. Biol. Chem.* **264,** 15893–15899
23. Jennings, M. L., and Passow, H. (1979) *Biochim. Biophys. Acta* **554,** 498–519
24. Nigg, E. A., and Cherry, R. J. (1979) *Biochemistry* **18,** 3457–3465
25. Golan, D. E., Brown, C. S., Cianci, C. M. L., and Furlong, S. T. (1986) *J. Cell Biol.* **103,** 819–828
26. Chang, S. H., and Low, P. S. (2001) *J. Biol. Chem.* **276**, 22223–22230
27. Evans, E., Mohandas, N., and Leung, A. (1984) *J. Clin. Invest.* **73,** 477–488
28. Discher, D. E., Mohandas, N., and Evans, E. A. (1994) *Science* **266,** 1032–1035
29. Discher, D. E., and Mohandas, N. (1996) *Biophys. J.* **71,** 1680–1694
30. Hiraoka, Y., Sedat, J. W., and Agard, D. A. (1987) *Science* **238,** 36–41
31. Bessis, M., and Mohandas, N. (1975) *Blood Cells* **1,** 307–313
32. Mohandas, N., Chasis, J. A., and Shohet S. B. (1983) *Semin. Hematol.* **20,** 225–242
33. Mohandas, N., and Chasis, J. A. (1993) *Semin. Hematol.* **30,** 171–192
34. Bennett, V. (1983) *Methods Enzymol.* **96,** 313–324
35. Fairbanks, G., Steck, T. L., and Wallach, D. F. H. (1971) *Biochemistry* **10,** 2606–2617
36. Van Dort, H. M., Moriyama, R., and Low, P. S. (1998) *J. Biol. Chem.* **273,** 14819–14826
37. Michaely, P., and Bennett V. (1993) *J. Biol. Chem.* **268,** 22703–22709